Crustal structure of the Labrador Sea conjugate margin and implications for the formation of nonvolcanic continental margins

Deping Chian[1] and Keith E. Louden

Department of Oceanography, Dalhousie University, Halifax, Nova Scotia, Canada

Ian Reid

Geological Survey of Canada (Atlantic), Bedford Institute of Oceanography, Dartmouth, Nova Scotia, Canada

Abstract. Wide-angle seismic studies have determined the detailed velocity structure along a 350-km-long profile across the Labrador margin. Combination of this model with a previously published cross section for the southwestern Greenland margin constitutes the first combined conjugate margin study based on seismic velocity structure. The results indicate three distinct zones across the Labrador margin, similar to the structure of the conjugate Greenland margin. Zone 1 represents 27 to 30-km-thick continental crust thinning gradually seaward over ~100 km distance. Farther seaward, zone 2 is 70-80 km wide, characterized by a distinct lower crust, 4-5 km thick, in which velocity increases with depth from 6.4 to 7.7 km/s. Interpretation for this lower crustal block favors an origin by serpentinized peridotite rather than by magmatic underplating. Zone 3 represents two-layered, normal oceanic crust. The cross sections from both margins are reconstructed to an early drift stage at Chron 27. This demonstrates that the serpentinites in zone 2 are symmetrically distributed between previous identifications of Chrons 31 and 33 on both margins. Zone 1 shows a marked asymmetry, with a gradual thinning of continental crust off Labrador contrasted with a rapid thinning off Greenland. The abundant serpentinization of upper mantle peridotite in zone 2 and the asymmetric shape of zone 1 are both probably related to a very slow rate of continental rifting which produced little if any melt.

Introduction

The details of the rifting mechanism on nonvolcanic, passive continental margins have remained elusive. This is apparent not only in the question of pure shear [McKenzie, 1978] versus simple shear [Wernicke, 1985; Lister et al., 1986] models [e.g., Le Pichon and Barbier, 1987; Boillot et al., 1989b, 1992; Keen et al., 1989, 1994; Sibuet, 1992], but also in the uncertainty whether a thin, high-velocity lower crust observed beneath the outer part of many nonvolcanic, rifted continental margins [e.g., Whitmarsh et al., 1986, 1990; Reid and Keen, 1990; Pinheiro et al., 1992; Chian and Louden, 1994; Reid, 1994] is due to serpentinized mantle or to magmatic underplating.

Proper study of the rifting mechanism requires understanding of the present crustal structure across the complete transition from continent to ocean on conjugate margin pairs. This can be accomplished by deep multichannel reflection profiling and wide-angle seismic refraction methods. While numerous reflection studies have been conducted on continental margins, few reflection data sets [Keen et al., 1989, 1994] exist across both conjugate margins. Of the refraction profiles which have been re-

ported for nonvolcanic continental margins, none have been conducted on both conjugates.

We present the first detailed crustal velocity cross section for a nonvolcanic conjugate margin pair and delineate the predrift crustal configuration during the continental stretching and separation. The new data include a 350-km-long wide-angle seismic refraction profile across the entire Labrador margin and two interesting refraction profiles, one along the shelf and the other one along the slope (Figure 1). These profiles are nearly conjugate to the two previous refraction lines on the SW Greenland margin [Chian and Louden, 1992, 1994] and are complemented by a coincident multichannel reflection profile [Keen et al., 1994]. Some of the major objectives of the refraction profiles on the Labrador margin are (1) to determine the velocity structure of the stretched continental crust; the relative thinning of upper and lower crust, when compared to its conjugate, may help indicate whether initial extension occurred primarily by pure or simple shear; (2) to determine the position and nature of the continent-ocean transition; does a thin layer of anomalously high-velocity lower crust, as observed on the conjugate SW Greenland margin, also exist on the Labrador margin and, if so, does it represent serpentinized mantle or magmatic underplating; and (3) to determine a combined, reconstructed cross section across both rifted margins at the start of seafloor spreading and at the time of final continental breakup.

This paper concentrates on determination of the crustal velocity structure across the Labrador margin from analysis of refraction profiles. Implication for the margin formation is made by comparison to the previously determined velocity model for

[1] Now at Geological Survey of Canada (Atlantic), Bedford Institute of Oceanography, Dartmouth, Nova Scotia, Canada.
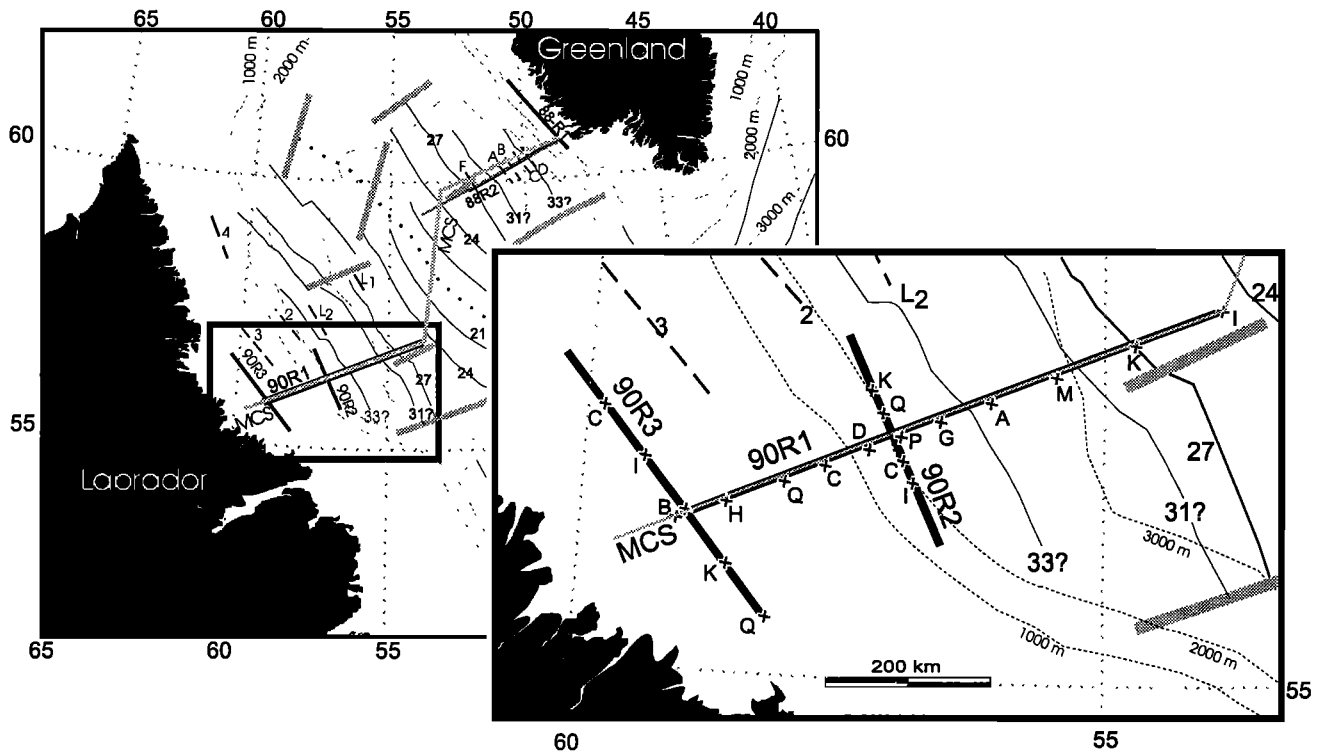
Figure 1. Map of the Labrador Sea, showing locations of new (this paper) and previous [*Van der Linden*, 1975; *Stergiopolous*, 1984; *Chian and Louden*, 1994] refraction profiles (thick solid or dashed); deep multichannel seismic (MCS) reflection lines (thin grey [*Keen et al.*, 1994]); fracture zones (thick grey); magnetic chrons (thin solid); bathymetric contours (thin dashed, in meters); and extinct rift (thick dotted) [*Bell*, 1989]. The inset diagram corresponds to the frame inside the larger map. Labeled crosses are ocean bottom seismometer (OBS) positions.

the Greenland margin, including a reconstruction of the two profiles at the start of normal seafloor spreading. The reconstruction of the crustal cross sections at the time of final continental breakup and the nature of the rifting process are developed by *Chian et al.* [1995], who combine data from both refraction and multichannel seismic (MCS) reflection profiles.

The Labrador Sea

The Labrador Sea is a northwestward extension of the North Atlantic Ocean, with the main basin about 900 km wide, bounded on the west by Labrador, on the east by SW Greenland, and on the north by Davis Strait (Figure 1). Its coastlines span a length of ~1300 km from their southern limits to Davis Strait in the north. The continental shelf and slope are much narrower on the western Greenland margin than on the Labrador margin. About 4 x10^6 km^3 of Cretaceous, Tertiary, and Quaternary clastic sediments have been deposited into the basin [*Balkwill*, 1987; *Tucholke*, 1988]. The crust is deeply subsided under the Labrador shelf, partly due to sediment loading, whereas little or no subsidence has occurred under the western Greenland shelf [*Rolle*, 1985].

The rift-related Mesozoic extension of the Canada-Greenland continent possibly started as early as ~160 Ma, as evidenced from the dating of coast-parallel dike swarms in SW Greenland [*Watt*, 1969]. This rifting occurred with little volcanic activity,

leaving less than 800 m of synrift extrusive basalts on the Labrador margin [*Balkwill*, 1987]. The subsequent seafloor spreading history of the Labrador Sea is documented by magnetic lineations, with well-defined anomalies observed between Chrons 21 and 27 (48-62 Ma) (Figure 1) [*Srivastava*, 1978; *Roest and Srivastava*, 1989]. Anomaly lineations older than Chrons 24-25 (54-57 Ma) are broken by several fracture zones, which are associated with a NW rotation of the spreading axis at anomalies 24-25, when Eurasia separated from Greenland. The less clearly defined, low-amplitude anomalies in areas older than Chron 27 have been interpreted by *Roest and Srivastava* [1989] and *Srivastava and Roest* [1995] as Chrons 31 (65 Ma) and 33 (78 Ma). This is in conflict with interpretations by *Chalmers* [1991] and *Chalmers and Laursen* [1995], who, on the basis of reprocessed MCS reflection data, suggest an initiation of seafloor spreading at Chron 27 (62 Ma). Their interpretation places the continent-ocean boundary (COB) ~120 km farther seaward of the previously suggested position.

A high-velocity lower crust that extends seaward of the continental slope for 70-80 km across the SW Greenland margin has been interpreted as serpentinized peridotite [*Chian and Louden*, 1994]. A similar high-velocity lower crust is also observed sporadically on older refraction data (Figure 1) on the SW Greenland margin [*Stergiopolous*, 1984] and on the northern Labrador margin [*Van der Linden*, 1975]. More data are needed to delineate the distribution of this material and to understand the processes involved in its formation.
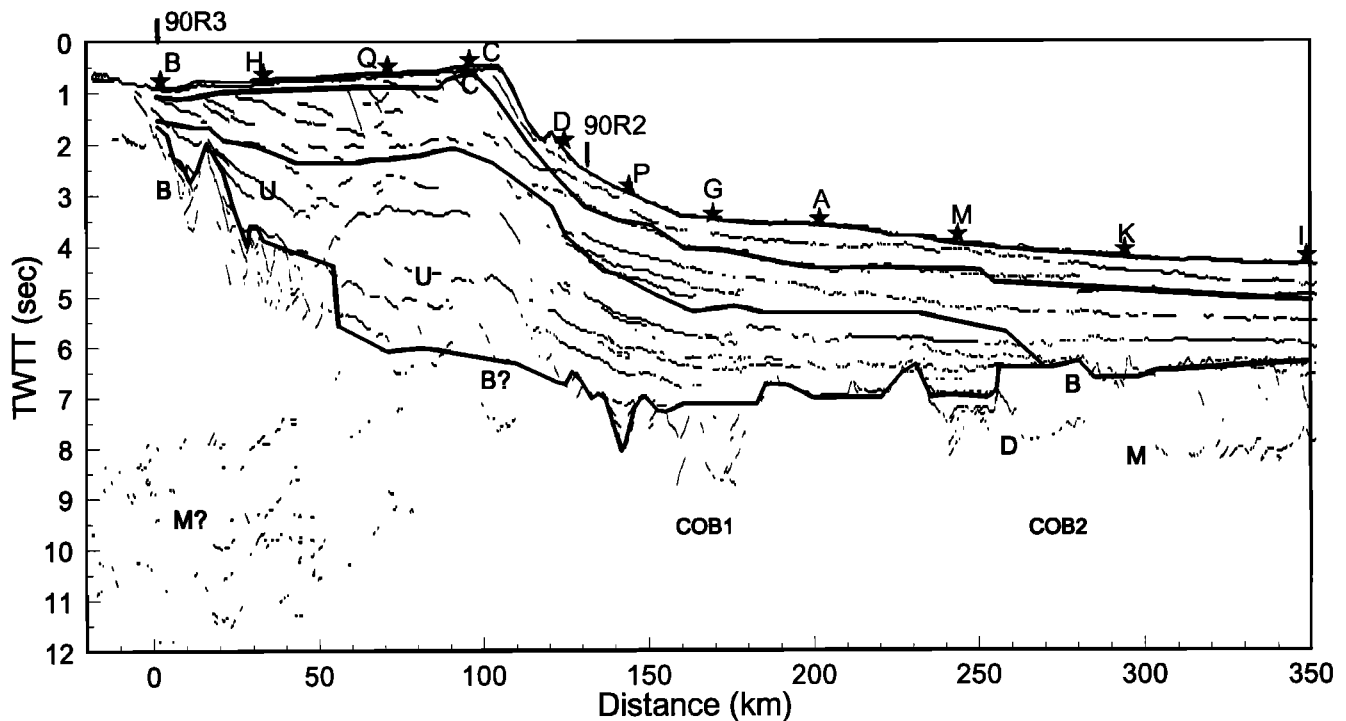
Figure 2. Line drawing from coincident multichannel reflection line 90R1 [*Keen et al.*, 1994]. Horizontal distance is consistent with what is used for wide-angle modeling. Labeled stars are OBS locations. Vertical arrows mark locations of two crossing refraction lines 90R2 and 90R3. U, "U" unconformity; B, basement; D, marks of intracrustal reflections; M, Moho. COB1 and COB2 are two possible positions for the continent-ocean boundary as identified by *Keen et al.* [1994].

Labrador Margin Seismic Data

Refraction Profiles

Three refraction profiles (90R1, 90R2, and 90R3) on the Labrador margin were shot in 1990 during CSS Hudson cruise 90-013 (see Figure 1 and Table A[1] for locations). The primary line is 90R1, which extends for 350 km across the entire Labrador margin. Shots from a 6×16.4L (6×1000 inch^3) air gun array were fired every 60 s for a shot interval of ~120 m. This refraction profile complements the coincident deep multichannel reflection profile of *Keen et al.* [1994] (Figure 2). The velocity structures obtained from line 90R1 are tied to results from a 150-km-long refraction profile 90R2, along-strike on the continental slope, and a 200-km refraction profile 90R3 along the shelf (I. D. Reid, manuscript in preparation, 1995).

A total of 21 ocean bottom seismometers (OBS) were used to record the three refraction profiles. Seismic signals from hydrophone and 4.5-Hz vertical geophones were recorded on cassette tapes. These analog data were digitized and interpolated to a fixed sampling rate of 100 samples per second. Corrections were made for OBS clock drift and shot delay. Corrections for both OBS positions and timing were determined by iteratively comparing observed and computed water wave arrivals. Further processing includes band-pass filtering of 4-8 Hz, clipping of high amplitudes, gain increasing linearly with horizontal range, and coherency mixing [*Chian and Louden*, 1992] of five adjacent shots scanned at velocities of 2.5-8.5 km/s for P waves and 2.5-4.5 km/s for S waves.

Coincident Multichannel Reflection Profile

We briefly review the Labrador segment of the MCS profile of *Keen et al.* [1994]. This profile (Figure 2) is coincident with the cross-margin line 90R1 and the sediment and basement structure were used for the subsequent refraction modeling. The sedimentary section can be divided into synrift and postrift units, separated by a breakup unconformity "U". This interpretation is tied to the regional seismic stratigraphy based on boreholes [*Bell*, 1989]. The U reflector corresponds to the top of the Bjarni formation of late Albian age (~98 Ma; >Chron 34). The synrift unit below U is discontinuous and occupies structurally low regions between basement blocks. The identification of U becomes less certain near the shelf break and below the slope.

Basement ("B") has been dissected by faults, some of which also cut the synrift sediments (e.g., the basement high between 10 and 25 km). From ~50 km, the depth of basement deepens sharply seaward by ~1.2 s, allowing thick synrift sediments to be deposited. Below the continental slope, basement reflections define a rough surface below a few relatively flat-lying sediment layers. Between 185 and ~240 km, a basement without any intracrustal reflections is observed. Farther seaward, another reflector bearing a basement character emerges at a depth of ~1 s shallower, underlain by subbasement reflections "D". This new basement has a typically oceanic hyperbolic reflection character.

The sedimentary line drawing of the reflection data was used to construct a preliminary two dimensional (2-D) velocity model for modeling the OBS data, by converting the two-way travel times (TWTT) to depth using an assumed velocity-depth relation. This relation was updated during the wide-angle modeling. The solid lines in Figure 2 are the sediment and basement boundaries, converted from the final 2-D velocity model. The seafloor and two sediment boundaries in the 2-D model closely follow the reflective events, with exceptions under the shelf where the events are more discontinuous. Location of the basement between distances of 50 and 120 km, where reflections are ambiguous, was adjusted during the modeling to agree with both the reflection and wide-angle data sets.

Moho reflections (M) are observed at both ends of the line: beneath the inner shelf at distances <50 km and at the eastern end of the line at distances >300 km. The seaward Moho is well recorded, while on the shelf near the base of the crust there are several reflectors with differences in TWTT of up to 2.5 s. When converted to depth, this amounts to a difference of 9 km assuming a lower crustal velocity of 6.9 km/s. Therefore it is difficult from reflection data alone to determine which reflector corresponds to the Moho.

Two-Dimensional Seismic Modeling

Useful wide-angle seismic phases observed in the OBS refraction experiment can be broadly divided into five categories, based on the layers through which the waves travel. To avoid ambiguity, we use the same labeling convention for all the data on line 90R1, regardless of the crustal type. The first phase is the direct water wave (P_w), traveling from the surface through the water column to the OBS on the seafloor. The second group consists of phases traveling through the sediments as refractions (P_1) or wide-angle reflections (P_1P) from the sediment/basement interface. It is generally easy to distinguish sediment phases from a third group, upper crustal phases P_2 (refractions) and P_2P (reflections), based on changes in apparent velocity. The fourth
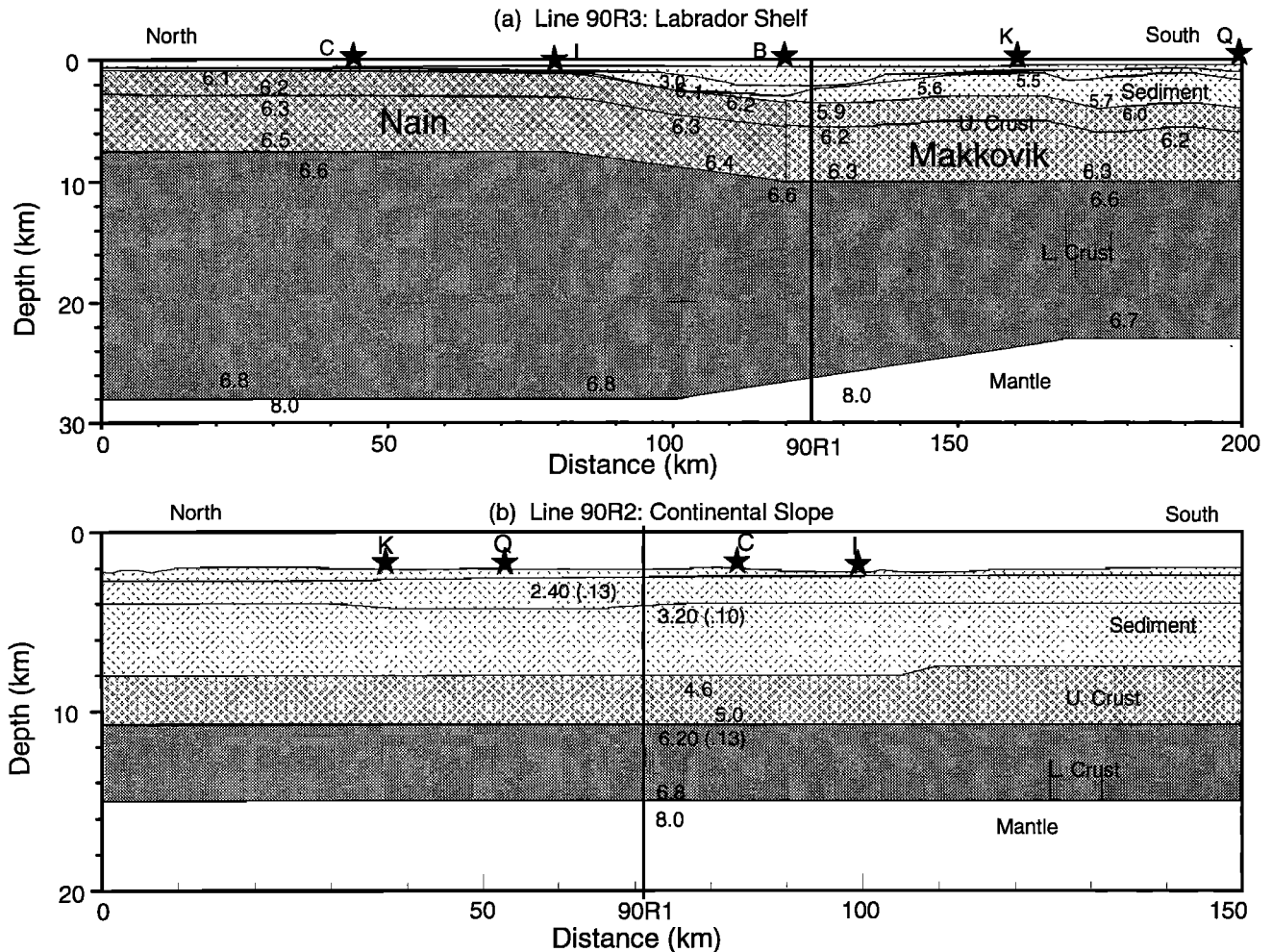
Figure 3. Velocity model for refraction lines (a) 90R3 and (b) 90R2. Solid stars represent OBS locations. Labeled vertical lines indicate intersection of profile 90R1. Numbers within each layer represent the velocity at the top boundary of the layer and the velocity gradient (shown inside brackets).

group is P_3, refracted in the lower crust, and P_mP, reflected from the Moho. The last phase is the mantle refraction, P_n, which has the highest apparent velocity of ~8.0 km/s, and is commonly distinct from crustal phases. Of the many recorded multiples, water and sediment multiples are usually the strongest, especially on line 90R1. Water multiples are denoted by appending a superscript to the notations for corresponding first arrivals (e.g., P_2^2) and sediment multiples are denoted by appending a prime (e.g., P_2'). This convention follows the notation of Chian and Louden [1994]. While it is possible that water multiples can be formed either at the source or receiver positions, modeling shows that most of the observed water multiples on line 90R1 were generated at the OBS receivers.

We use a simplified 2-D ray-tracing algorithm [Reid, 1994] for generating an initial 2-D velocity model that results in an overall travel time fit to observed seismic phases. The model was then refined by use of the SEIS83 algorithm [Cerveny et al., 1977], which can better describe the complex 2-D structure with velocity contours rather than individual layers and enables us to image both conjugate margins using the same method as that of Chian and Louden [1994]. Two horizontal scales will be used. Ranges represent the distance between shots and a particular OBS, while distances refer to the positions of the OBS and shots on the 2-D model. Generally, the observed OBS record sections and computed travel times are plotted together with the ray paths

on the 2-D velocity model. However, when only minor lateral velocity variations are present, we include synthetic seismograms rather than the ray paths and the velocity model. Owing to space limitations, only the most important profiles are shown in the text. For a complete description of the abundant data set used, readers are referred to Chian [1994] or the electronic supplement appendix of this paper.

Strike Lines 90R2 and 90R3

The OBS data along line 90R3 have been modeled by I. D. Reid (manuscript in preparation, 1995) with a two-layer crust underlying a thin sheet of sediments along the shelf (Figure 3a). A clear velocity contrast at a distance of 80 km is evident in the upper crust. North of this point, the upper crust is described by a velocity of 6.3 km/s at ~0.9 km depth with a downward gradient of 0.05 s⁻¹. To the south, the upper crust thins and its velocity decreases to 6.0 km/s at 3-4 km depth with the same gradient. This velocity contrast is comparable with the upper crustal structure along the SW Greenland shelf [Chian and Louden, 1992]. The higher upper crustal velocities north of OBS I are associated with a magnetic low similar to those which characterize the Nain plutonic suite [Bell, 1989]. The tectonic front between the Nain (Archean) and the Makkovik (Proterozoic) provinces occurs approximately at OBS B, but there does not appear to be any significant variation in crustal velocities at this boundary. Below
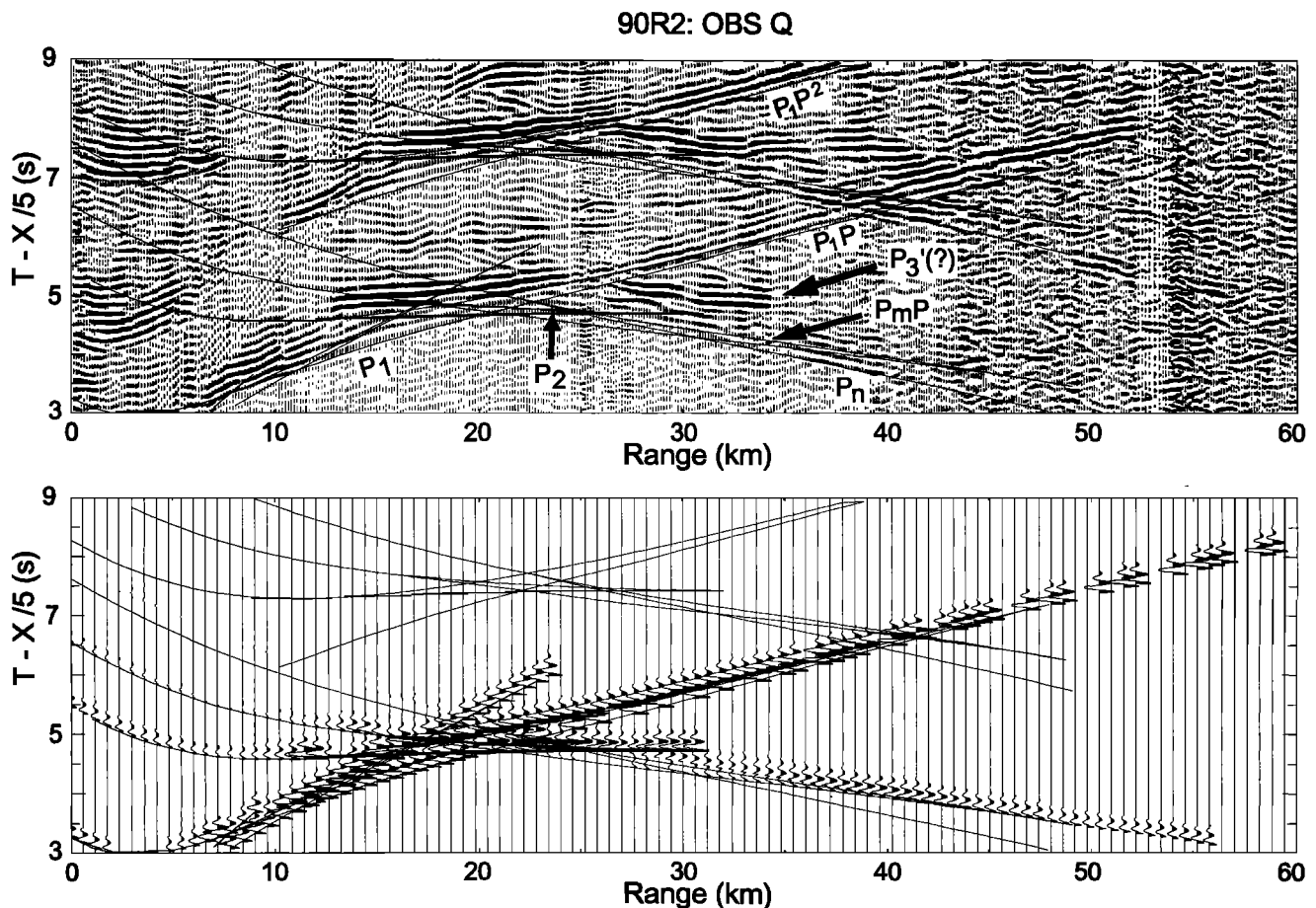
Figure 4. (top) Wide-angle record section and computed travel time curves at OBS Q on line 90R2. Processing includes band-pass filtering of 4-8 Hz, clipping of high amplitudes, gain increasing linearly with horizontal range, and coherency mixing [Chian and Louden, 1992] of five adjacent shots scanned at velocities of 2.5-8.5 km/s. See text for description of phase labeling. (bottom) Asymptotic ray synthetic seismograms of OBS Q.

6.5-7 km depth, the lower crust has a velocity of 6.6 km/s with a downward gradient of 0.02 s^{-1}. Unlike the lower crustal structure in the SW Greenland margin, there is no seismic evidence for a velocity boundary below 7 km. The Moho is well modeled by clear P_mP and P_n phases on several OBS, showing a Moho depth of 29 km in the north and 27 km in the south.

Refraction line 90R2 is oriented along strike on the continental slope of the Labrador margin. The purpose of this line was to obtain a well-controlled velocity structure beneath the thick sediments of the continental slope, which can help to constrain modeling of cross line 90R1. The available data include four OBS (K, Q, C, and I) and a coincident single-channel reflection profile (Figures 4 and A1-A5). The reflection profile contains useful data from only the top part of the sediments (TWTT of less than 4 s) and is used for specifying the first three layers in the 2-D model [*Chian*, 1994]. Deeper velocity structures are obtained from modeling the sediment and basement arrivals. Velocity in the sediment is well-defined by strong phases P_1 and P_1P, which are well recorded at OBS Q (Figure 4) and OBS 1 and C (Figures A4 and A5). The water multiples (P_1^2 and P_1P^2) of these two phases are equally well-defined in OBS Q and I. This is best modeled by a thick sediment layer with a velocity of 3.0-3.6 km/s at 4.5-8.0 km depth.

Beneath the sediments, a two-layer structure is evident for the crust. Travel time and amplitude modeling requires that the upper crust has a relatively low velocity of 4.6-5.0 km/s with a gradient

of 0.1 s^{-1}. A higher velocity for this layer would cause the P_2 phase to arrive too early between ranges of 22 and 28 km at OBS Q (Figure 4). For the lower crust, there are ambiguities as to whether the wide-angle reflection from the Moho is the discontinuous phase labeled P_mP or the later phase labeled P_3'. In the latter case, it is difficult to fit P_n with a reasonable crustal model which can be tied to profile 90R1. In the first case, however, the modeled lower crust matches well with the cross profile 90R1, with a velocity of 6.2-6.8 km/s at 10.5-14 km. This final velocity model is shown in Figure 3b.

Cross Line 90R1

Refraction line 90R1 has 11 OBS deployed over a distance of 350 km across the Labrador margin. It intersects profile 90R3 close to the boundary between the Nain and Makkovik provinces (Figure 3). In the following sections, we describe the major features of the record sections shown and relate them to the velocity model. From the inner shelf to the shelf break, major constraints on velocities are obtained from OBS H (Figure 5) and Q (Figure 6). Farther seaward, results from profile 90R2 are used during the modeling of OBS D (Figure A8), P (Figure 7), and G and A (Figure 8). On top of the oceanic basement, the last two OBS at the eastern end of the profile, K (Figure A11) and I (Figure 9) show very good data quality, including clear water multiples and S waves.
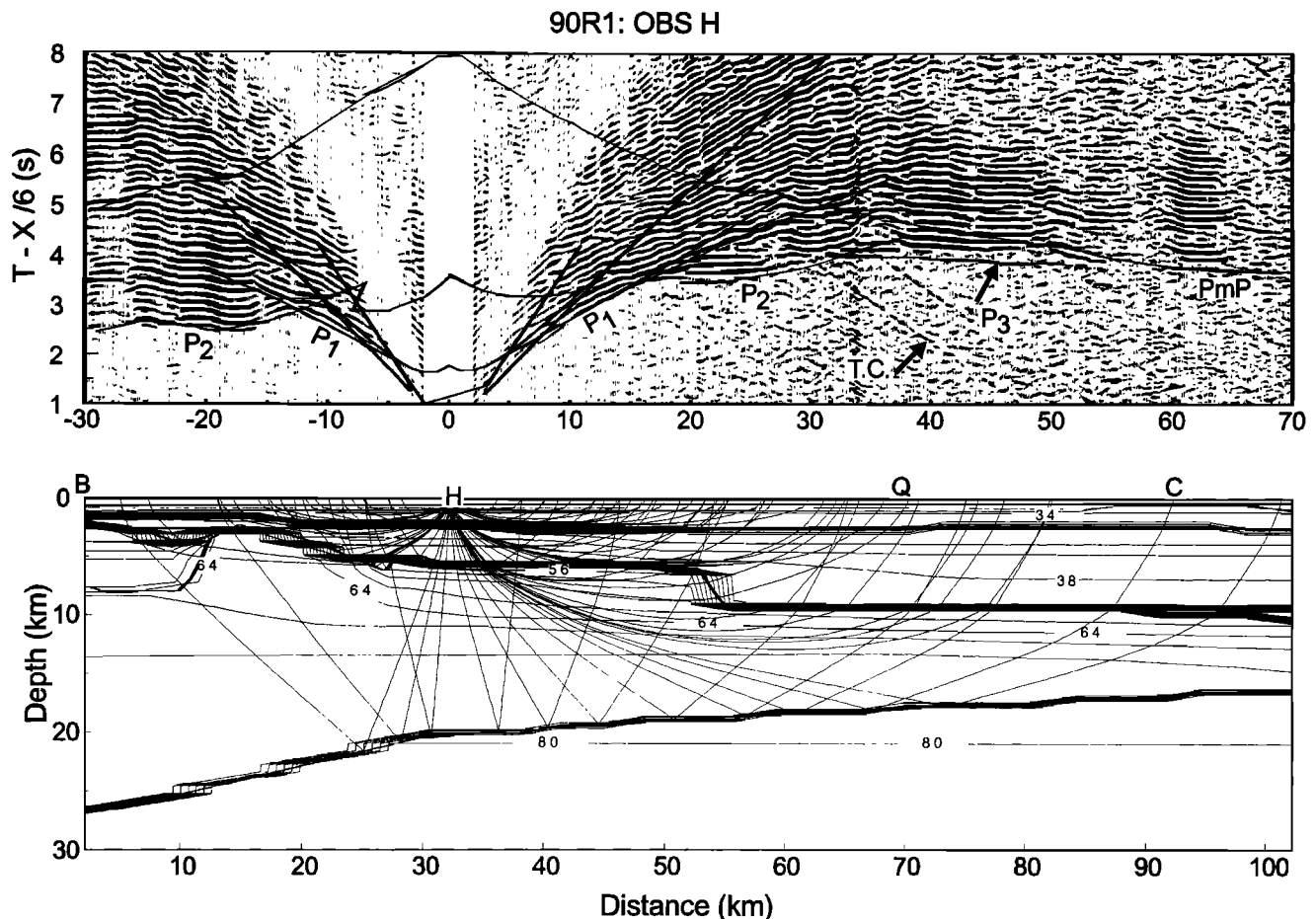
Figure 5. (top) Wide-angle record section and computed travel time curves at OBS H on line 90R1. See caption of Figure 4 for processing steps. (bottom) Velocity model and selected ray paths for generating travel time curves.
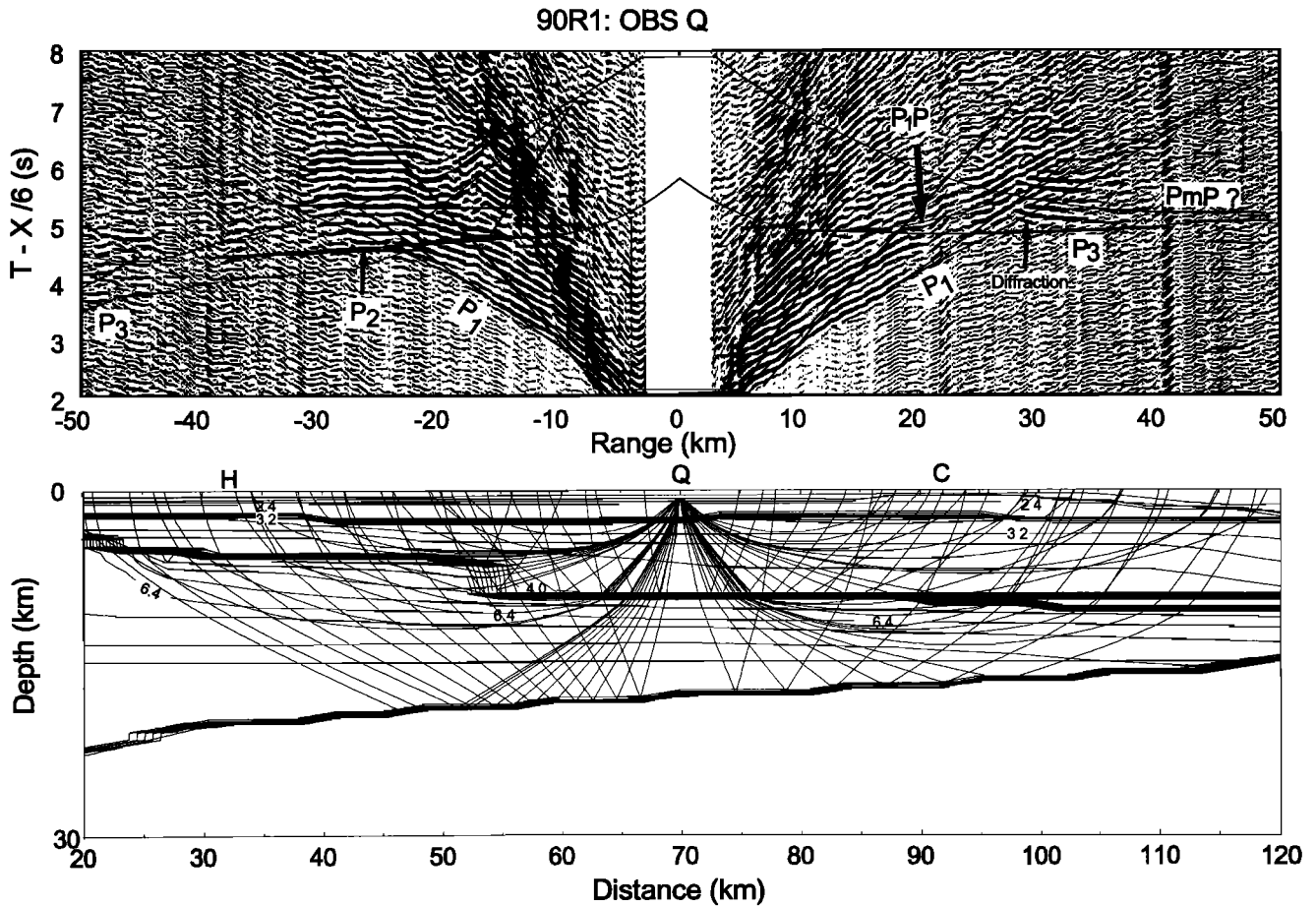
Figure 6. (top) Wide-angle record section and computed travel time curves at OBS Q on line 90R1. See caption of Figure 4 for processing steps. (bottom) Velocity model and selected ray paths for generating travel time curves.

OBS H. Between -10 km and -30 km range, the curvature of P_2 is well modeled by the existence of a 6.4 km/s intrusion between distances of 15 and 20 km. This feature is observed in the reflection profile (Figure 2). Between 20 and 30 km range, the curvature of P_2 is modeled by an abrupt change in basement depth at 52 km distance. This feature is supported by the reflection data, which show a change of reflectivity pattern. Between 38 km and 50 km range, a strong and continuous phase P_3 defines the crustal velocity as 6.2-6.9 km/s (Figure 5b). P_mP is visible at 55-70 km range, modeled by a Moho at a depth of 18 km at a distance 67-77 km. For distances <67 km, the Moho depth is determined by gravity modeling, as discussed later.

OBS Q. The abrupt change in basement depth at 52 km distance produces a time shift of 0.3-0.4 s for P_2 and P_3 at ranges of -40 km to -22 km from OBS Q (Figure 6). Despite the crustal complexities to the west of the OBS, the travel time and slope of P_2 (strong at ranges -30 km to -20 km) are well modeled. To the east of the OBS, refractions (P_1) from the ~9-km-thick sediments are clearly recognizable at ranges up to 32 km. The modeling of P_1 on both sides of the OBS indicates a velocity gradient of 3.2-4.0 km/s for depths of 2.5-9 km. The reflection from the sediment/basement interface (P_1P) arrives later than P_1 due to the large sediment thickness. To model P_1P, we used the coincident reflection profile, which shows a few strong reflectors fading out below a TWTT of 5.5-6.0 s (Figure 2). This gives a few options for choosing the basement interface and the one that produces the

best overall fit is chosen for the final model. This choice also produces a consistent travel time for P_1P^2 on the adjacent OBS D (Figure A10).

There is no evidence on OBS Q to suggest more than one layer for the crust. A proper extension of lower crustal velocity contours from both sides of the OBS produces a reasonable fit to P_3 except for the curvature of its hyperbola diffraction at ~30 km range. There is little control on the depth of the Moho from this OBS, as P_mP cannot be convincingly determined.

OBS P. On OBS P (Figure 7), a strong sediment phase P_1 between ranges of ±40 km reveals a sediment velocity structure which is consistent with adjacent OBS D (Figure A12) and the nearby along-strike refraction profile 90R2. For the crust, a two-layer structure, as determined from profile 90R2, is consistent with phases P_1P, P_2, P_2P, and P_3 at positive ranges from OBS P. P_1P is visible at 10-20 km range, with a slope that corresponds to a slightly higher apparent velocity than P_1. P_2P is well modeled at ranges of 8-12 km and 20-30 km.

Modeling of similar phases from adjacent OBS on profiles 90R1 and 90R2 supports the existence of an upper layer, with a velocity of 4.8-5.0 km/s and a distinct lower layer with velocity of 6.2-6.9 km/s, extending westward to join the single layer crust beneath the shelf. P_mP is not visible at OBS P, but there is a strong P_n phase. This P_n phase is continuous with the P_3 arrival, with a change in slope at 37 km range. This phenomenon also exists for OBS G and A (Figure 8) and is attributed to an in-

90R1: OBS P
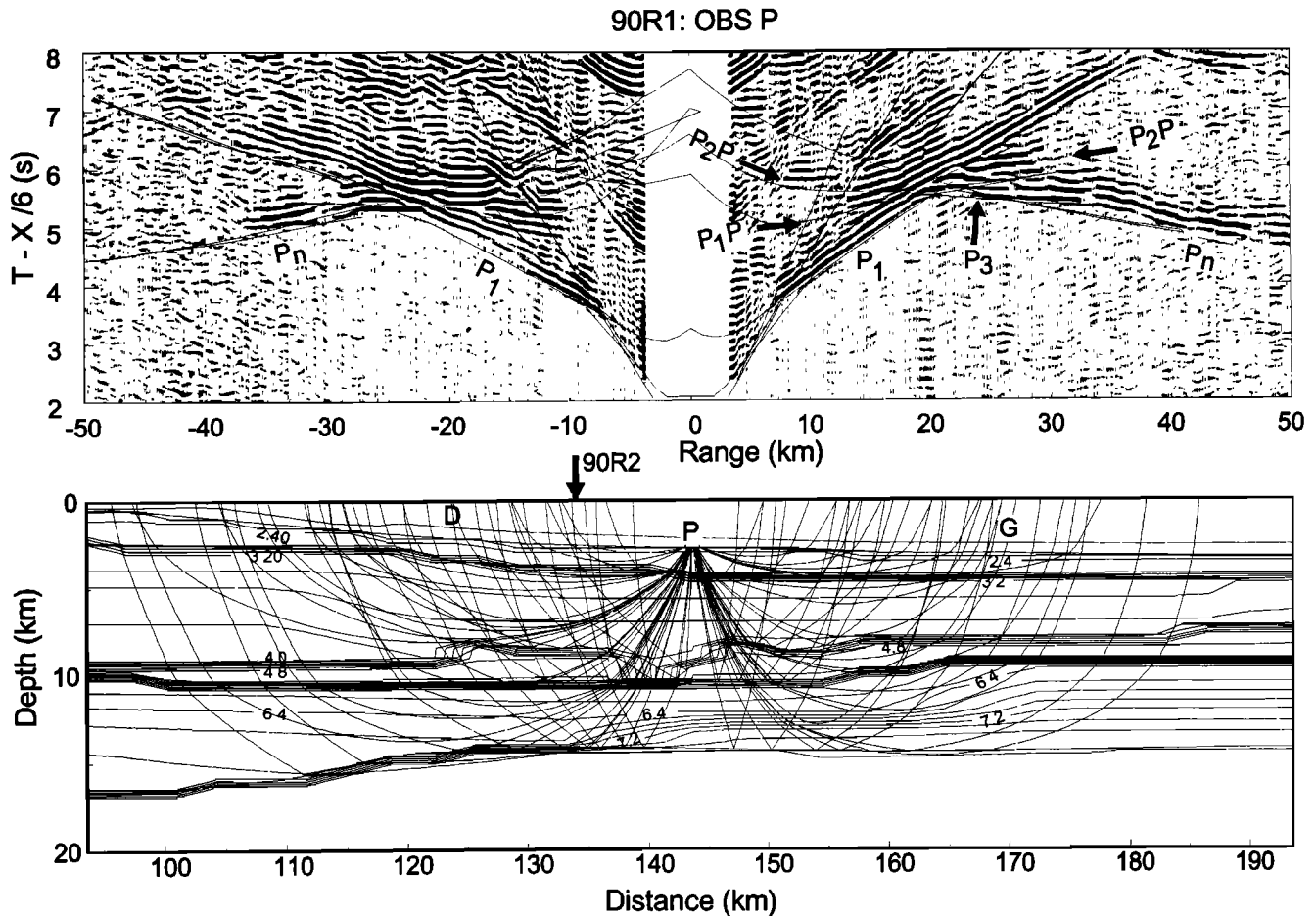
Figure 7. (top) Wide-angle record section and computed travel time curves at OBS P on line 90R1. See caption of Figure 4 for processing steps. (bottom) Velocity model and selected ray paths for generating travel time curves.

creased velocity gradient (0.1 s^{-1}) in the lower crust. This high gradient creates velocities of up to 7.7 km/s at the base of the lower crust.

OBS G and A. Modeling of P_1 at OBS A shows that the deep sediments to the east of OBS A (Figure A12) have velocities of 3.2-3.8 km/s, similar to velocities under adjacent OBS G (Figure 8a) and D (Figure A10). For the sediment to the west (Figure 8b), higher velocities of 3.3-3.9 km/s at distances of 185 km and 200 km are required to fit P_1. This slight increase of sediment velocity is consistent with the change in reflective pattern at a distance >180 km in the reflection profile (Figure 2).

The low-velocity upper crust still exists near OBS G as seen from a strong P_2P phase at ranges of 20-26 km. Well-defined crustal refractions are only observed as water multiples (P_3^2 and P_n^2). These two refracted phases are continuously linked, while the P_mP^2 phase is absent. This is similar to OBS P (Figure 7) and OBS A. On OBS A, crustal phases are observed only to the west. Although confused with the reverberations of P_3, P_2P can still be recognized as a group of amplitudes at a smaller apparent velocity from ranges of -15 km to -30 km. No clear crustal phases are observed to the east (Figure A12), consistent with the reflection data which show a transparent crust under and to the east of OBS A, and therefore we hypothesize that the low-velocity upper crust terminates at a distance of ~200 km. The lower crustal P_3 phase at OBS A and G is modeled with a velocity gradient from 6.4 km/s at the top to ~7.7 km/s at the Moho. As on OBS P (Figure

7) and G, there is no P_mP phase as P_3 merges with P_n. There are a few diffraction phases on OBS A that we could not model.

OBS I. The seismic phases recorded by OBS I (Figure 9) and K (Figure A15), show a pattern different from the OBS farther west. The modeling of these phases is relatively easy because the coincident reflection data has good control on the TWTT for the sediments, crust, and Moho. At OBS I, modeling of the sediment arrival P_1 indicates that the sediments have relatively low velocity of 2.2 km/s to 2.6 km/s between 4 and 5.5 km depth. A two-layer crust is necessary in order to model the change in slope from P_2 to P_3 at a range of 12 km, with upper crustal velocities of 5.6-6.0 km/s above 7.5 km depth and lower crustal velocities of 6.8-7.1 km/s. Clear S waves (S_1 and S_2) are observed only at OBS K and I. These S waves are doubly converted from and to P waves at the sediment/basement interface. S velocities in the crust can be best described by a Vp/Vs ratio of 1.82 (Poisson's ratio of $\sigma = 0.28$).

Velocity Model

The cross section (Figure 10c) for the Labrador margin can be divided from west to east into three zones, similar to the divisions observed on the SW Greenland margin [*Chian and Louden*, 1994].

Zone 1 represents a thinning of continental crust; its crustal structure is controlled by coincident reflection profile, OBS H, Q, and D, and gravity modeling. Beginning with a thickness of 27
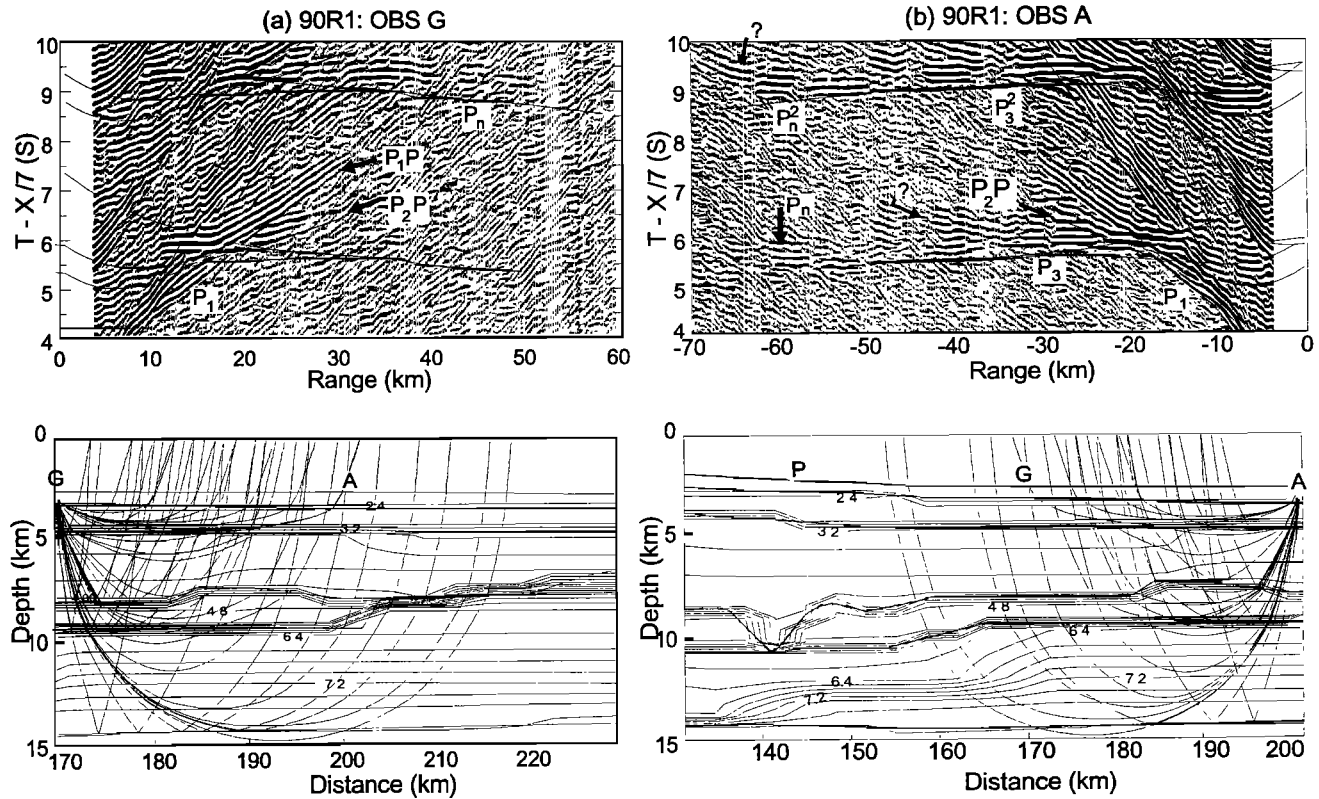
Figure 8. Wide-angle record section, computed travel time curves, and selected ray paths of (a) OBS G and (b) OBS A on line 90R1. See caption of Figure 4 for processing steps.

km at the western end of the model, the crust is reduced to a thickness of 13 km within a distance of 52 km. At this point, basement deepens abruptly. Farther seaward, the crust underlying the thickest (~9 km) sediments is characterized by a single layer with a velocity increasing smoothly from 6.2 km/s at the top to 6.9 km/s at Moho. Since this velocity gradient, when corrected for pressure differences, is different from that in adjacent upper crust at distances <52 km, the crust seaward of this point may be lower continental crust (M. Salisbury, personally communication, 1994), with upper continental crust terminating at ~52 km distance, consistent with a change in reflectivity and depth to basement in the reflection profile (Figure 2). Seismic modeling of the lower crust and Moho boundary also utilizes constraints from gravity models (see following section). The model is less well constrained from seismic data alone, since PmP arrivals are only sporadically distinguishable from reverberations and noise.

Zone 2 is characterized by a distinctive lower crust with an anomalous velocity structure of 6.4 km/s at 9.5 km to 7.7 km/s at 14.5 km depth. This lower crust is present between distances of 160 km and 250 km. The small velocity contrast at the Moho generates poor reflections on wide-angle and vertical-incidence profiles. Between distances of 100 km and 200 km, a relatively low-velocity (4.8-5.0 km/s) layer forms the upper crust. The existence of this 1 to 2-km-thick layer is well-defined from an along-strike line 90R2 (Figure 3) on the continental slope, as well as from OBS D, P, G and A on line 90R1.

Zone 3 has a 5.5-km-thick, two-layer crust with an oceanic character. The transition between zones 2 and 3 is a complex region between distances of 240 and 255 km, associated with a 1-km shallowing of basement and 3-km shallowing of the Moho.

East of 260 km, the basement surface becomes smoother, and the velocities and crustal thickness have little lateral variation. Here the upper crust is 1.8-2.0 km thick with a P velocity 5.6-5.8 km/s. The lower crust is 3.0-3.5 km thick with normal layer 3 velocity (6.8-7.0 km/s). The modeling of the well-defined S phases indicates a Vp/Vs ratio of 1.82 ($\sigma = 0.28$) for oceanic layers 2 and 3.

To estimate the possible errors associated with the crustal structure shown in Figure 10c, we use a method similar to that of Chian and Louden [1994]. In this method, the velocity and depth of a specific structural unit are perturbed, and the error bounds are determined based on the maximum allowable travel time misfit at a specific receiver (OBS). This method results in an estimated error bound of ±0.1 km/s for the lower crust in zones 1, 2, and 3 , assuming that the layers above are correct and the average maximum travel time misfit is 35 ms (Figure A18). This result is similar to error estimates for the Greenland margin [Chian and Louden, 1994]. In certain regions of the model, the structure is probably better defined than this estimate because additional information, such as constraints from the coincident reflection and gravity profiles, and overlapping of wide-angle ray paths from more than one OBS, improves the accuracy of the velocity model. On the other hand, there are poorly constrained regions in the model where the errors are greater than estimated (see question marks in Figure 10c) because of small ray path density. The low-velocity upper crust between 100 and 200 km distances has a dense ray coverage by both refraction profiles 90R1 and 90R2. However, since the seismic phases P2P and P2 are only defined over a limited horizontal range, the error bounds here are greater and estimated to be ±0.2 km/s. In addition, because PmP arrivals are only sporadically observed over the

90R1: OBS I
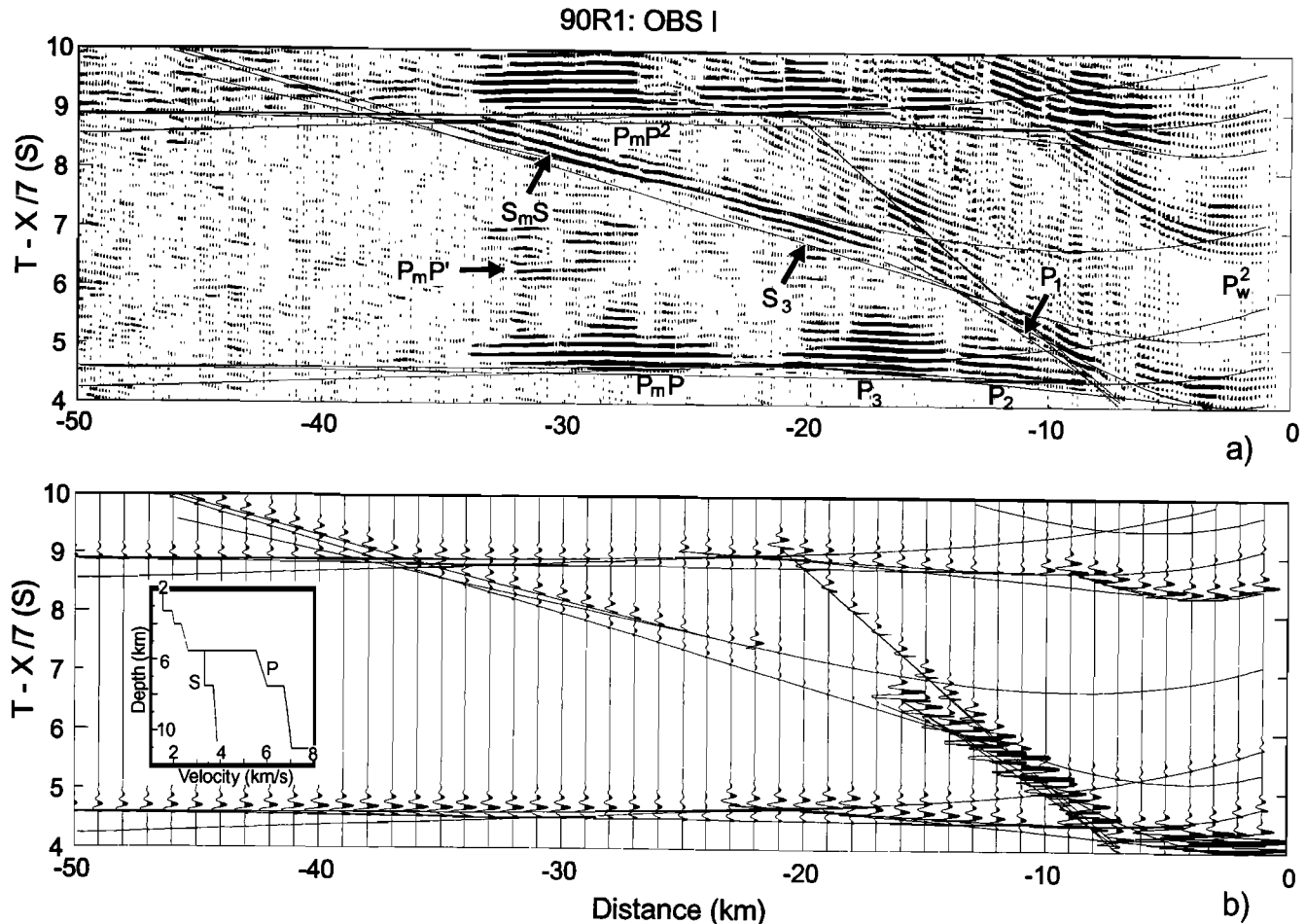
Figure 9. (top) Wide-angle record section and computed travel time curves at OBS I. See caption of Figure 4 for processing steps. (bottom) Synthetic seismograms generated from velocity model as outlined by the inset diagram.

region of 60 to 120 km on OBS H, Q, C and D, the nature of the Moho is undoubtedly more complex than represented by the large velocity contrast in the model.

### Gravity and Magnetic Modeling

We carried out gravity modeling based on the velocity section across the Labrador margin (Figure 10), assuming a velocity-density relationship and a reference level that are consistent with those previously used for the conjugate Greenland margin [*Chian and Louden*, 1994]. The water layer and the first two thin sediment layers for the Labrador margin are assigned a density of 1.03, 1.8, and 2.1 g/cm^3, respectively. To determine the density (ρ) for the remaining thick sediments whose velocity (v) lies between 3.2 and 4.0 km/s, we use a linear relation $\rho = 0.25\ v + 1.6$ for $v \in (3.2\text{-}4.0)$ km/s. When this is coupled with a density of 2.65 g/cm^3 for the low-velocity upper crust (4.0-5.2 km/s), and $\rho = -0.6997 + 2.2302\ v -0.598\ v^2 + 0.07036\ v^3 - 0.0028311\ v^4$ (*Ludwig et al.*, 1971; *Chian and Louden*, 1994] for the remaining crust, a general fit for zones 1 and 2 is obtained.

Major uncertainties exist in the gravity model, primarily because small changes in density for the thick sediments could produce significant changes in the computed gravity anomalies. For example, at 0-70 km distance, the refraction Moho (profile 90R3) is shallower than the reflection Moho interpreted by *Keen*

et al. [1994]. This difference is accommodated in our model by lower densities within the deeper sediments. Further uncertainties arise from the choice of Moho topography for the western end of the cross section where the Moho shallows toward the basin. We find that a good fit to the gravity anomaly is obtained by setting the continental crustal thickness to be 34 km. Because the computed anomaly is very sensitive to changes in depth of the Moho, we obtain the Moho relief between 0 and 70 km where there is little seismic control and where the sediments are not too thick to cause large uncertainty.

The resultant gravity model generates a gravity profile that fits the general features of the observed data (Figure 10b). However, as with zone 3 on the SW Greenland margin [*Chian and Louden*, 1994], the computed gravity anomaly near the eastern end of the profile is >20 mGal higher than observed. This suggests that either the actual density for the oceanic crust in zone 3 is lower than computed or the density in the oceanic lithosphere varies across the margin, as might be expected, given the age of the basin. The lack of control on lithospheric variations across the margin and the uncertainty in sediment densities leave us little confidence in making further improvements to the gravity fit by varying the crustal densities.

Figure 10a shows a plot of observed magnetic anomalies interpolated along the refraction line across the Labrador margin (refer to *Keen et al.* [1994]). The first clear magnetic anomaly is
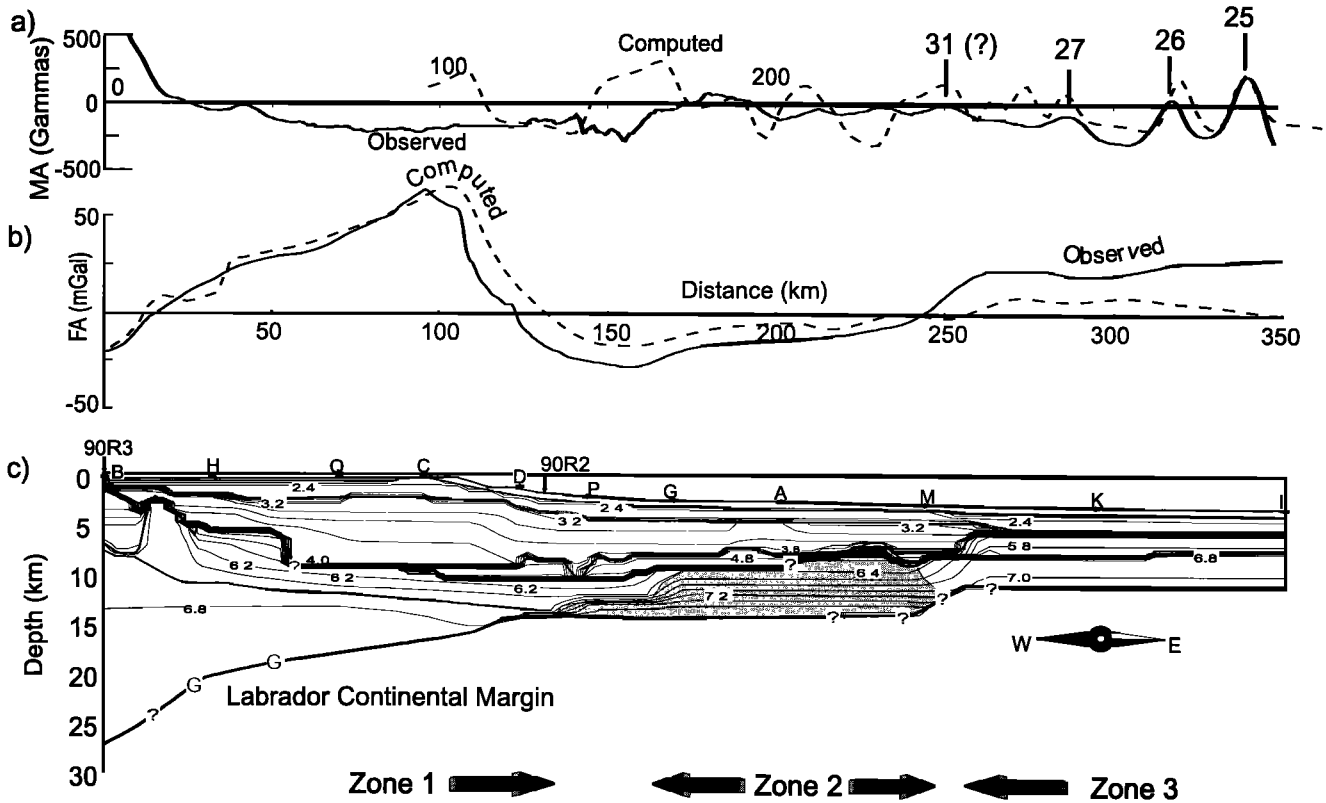
Figure 10. (a) Observed magnetic anomaly (solid line) and computed anomaly (dashed line) along profile 90R1. The spreading rate and direction are from *Roest and Srivastava* [1989] using the time scale *of Kent and Gradstein* [1986]. (b) Observed free air anomaly (solid line; from *Keen et al.*, [1994]) and computed gravity anomaly (dashed line) along profile 90R1 calculated from a 2-D density model derived from the velocity model (see text for details). (c) The 2-D velocity model showing contours of *Vp* (in kilometers per second) across the Labrador margin. The contour interval is 0.2 km/s. At some significant velocity boundaries (thick lines), contour lines are terminated for clarity. Labeled solid stars indicate positions of OBS. Zones 1, 2, and 3 represent continental, transitional, and oceanic crust. Vertical exaggeration is 3:1.

Chron 27 inside zone 3. Landward of this anomaly, a smaller-amplitude peak possibly represents Chron 31 [*Roest and Srivastava*, 1989], at the junction between zones 2 and 3 . The magnetic anomalies in zone 2, where the high-velocity lower crust is observed, are characterized by low amplitude oscillations, in a pattern different from that in zone 3 . Therefore, as with the interpretation of the SW Greenland margin [*Chian and Louden*, 1994], it is possible that the formation of true oceanic crust was initiated between Chrons 27 and 31 and that zone 2 represents a wide transition zone from the continent to the ocean.

Interpretation of Crustal Model

In this section, we present a mutually consistent interpretation of the velocity structures of both margins of the Labrador Sea. We will consider in particular the nature of the continent-ocean boundary and whether the high-velocity lower crust in zone 2 is formed by magmatic underplating or by serpentinization.

Nature of Continent-Ocean Boundary

There exists a wide (70-80 km) zone of crust (zone 2) with an anomalously high velocity across both Labrador and Greenland margins (shaded areas in Figure 11). When the positions of high-

velocity material are connected to form a band at each margin, this band approximately follows the northwestern trend of magnetic anomalies and covers crust older than Chron 31. This zone is characterized by a two-layer crust (Figure 12) with high-velocity gradient from 6.4 to 7.7 km/s in the lower crust (4-5 km thick), and low velocities (4-5 km/s) in the thin (1-2 km thick) upper crust.

A similar two-layer transitional crust is also observed on several other nonvolcanic rifted continental margins. For example, *Whitmarsh et al.* [1990] observed on the Iberia margin a significant velocity difference between normal oceanic crust and the high-velocity transitional crust and placed the COB at this seaward boundary. On the margins of Newfoundland, however, *Todd and Reid* [1989], *Reid and Keen* [1990], and *Reid* [1994] placed the COB at the landward boundary between normal continental crust and the high-velocity crust. These proposed positions of the COB approximately correspond to the two boundaries between zones 1, 2, and 3 in Figure 12. On the coincident reflection profiles of *Keen et al.* [1994], these two boundaries are associated with significant change in basement character (COB1 and COB2 in Figure 2).

We suggest that neither of these two discrete boundaries represents the true COB, but that the ocean-continent transition on conjugate margins of the Labrador Sea is best described by the
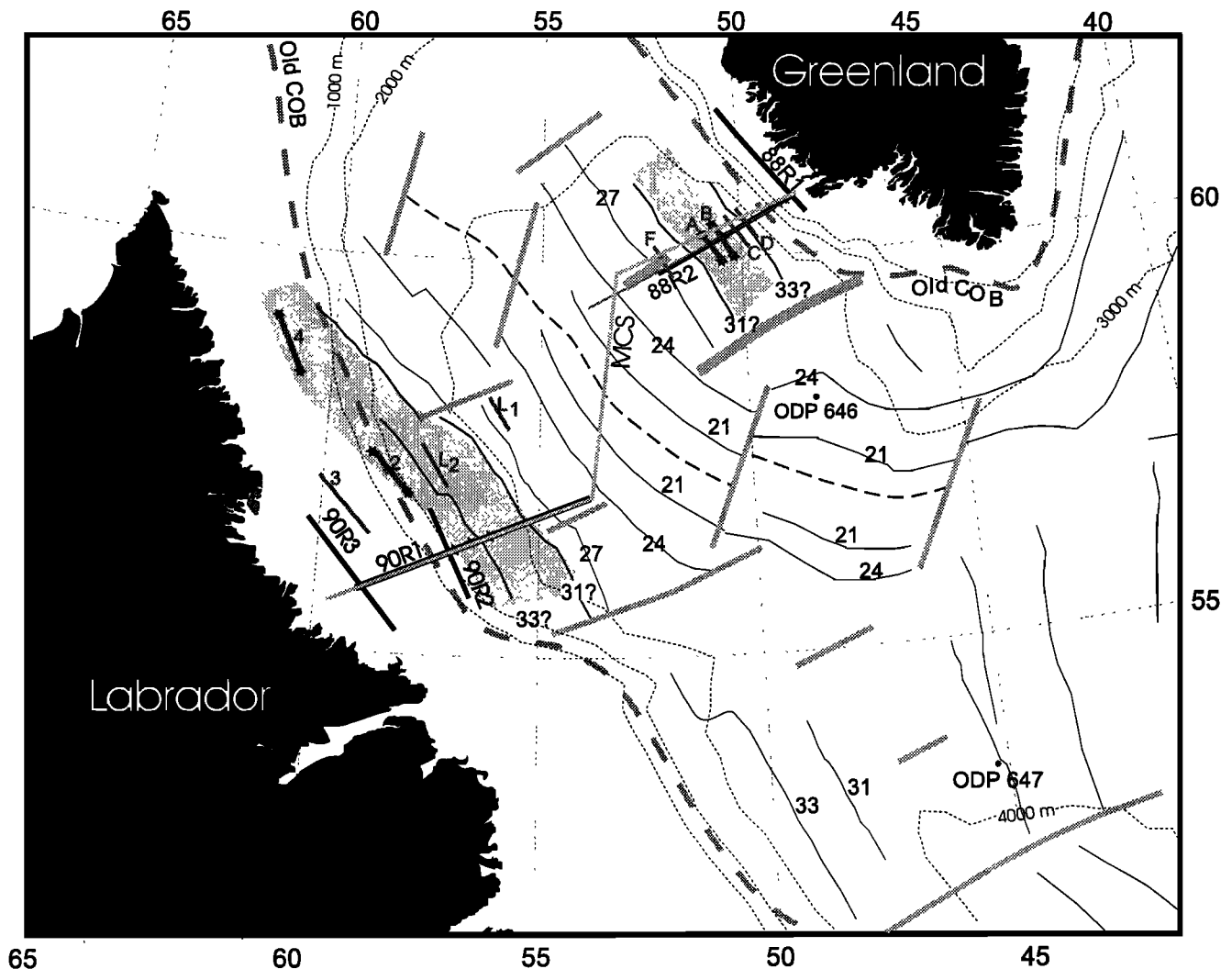
Figure 11. Map of the Labrador Sea, showing the generalized distribution of the high-velocity material (shaded area) on both margins. Solid stars represent locations of the OBS or sonobuoys which show evidence for a high-velocity lower crust. See caption of Figure 1 for further description of the map.

wide area of zone 2, rather than by a sharp boundary. The main reason for this interpretation is that the velocity structure of zone 2 is completely different from either the continental (zone 1) or oceanic crust (zone 3), and any a sharp COB would imply that the material of zone 2 is predominantly continental or oceanic in character. This interpretation is similar to the suggestion of *Whitmarsh et al.* [1993], who proposed that an ocean-continent transition (OCT) several tens of kilometers wide exists on the Iberia margin. It is possible that this OCT and the high-velocity zone on the conjugate margin of Newfoundland [*Todd and Reid*, 1989; *Reid and Keen*, 1990; *Reid*, 1994] are similar to zone 2 on conjugate margins of the Labrador Sea.

Setting zone 2 as a wide region between continental and oceanic crust implies that true seafloor spreading in the Labrador Sea started seaward of this zone at Chrons 27-31 [*Chian and Louden*, 1994]. This is consistent with the interpretation of *Chalmers* [1991] and *Chalmers and Laursen* [1995], based on reprocessed previous MCS reflection data across the western Greenland margin. The revised timing for the generation of true oceanic crust is younger than the previously suggested position at Chron 33 [*Roest and Srivastava*, 1989].

Origin of High-Velocity Lower Crust

As summarized by *Chian and Louden* [1994], the high-velocity (>7.2 km/s) transitional crust can be interpreted as either underplate (i.e., high-Mg mafic gabbro) [*Todd and Reid*, 1989; *Reid and Keen*, 1990; *Whitmarsh et al.*, 1990; *Keen et al.*, 1994] or undercrusted serpentinized peridotite [*Pinheiro et al.*, 1992; *Reid and Keen*, 1990; *Reid*, 1994]. Seismic velocities alone cannot definitely distinguish between these two models even when both P and S phases are observed [*Chian and Louden*, 1994]. Here we will try to combine other available observations with the velocity model and discuss the implications of each interpretation. It will be seen that while each of the two models explains some of the observed features, neither model can explain all the phenomena. However, in general, the serpentinite model is more consistent with observations than the magmatic underplating model.

Thickness. In the underplate model, a higher asthenospheric temperature is required to produce the observed high velocity by Mg enrichment [*Furlong and Fountain*, 1986; *White and McKenzie*, 1989]. At normal rates of continental stretching, this
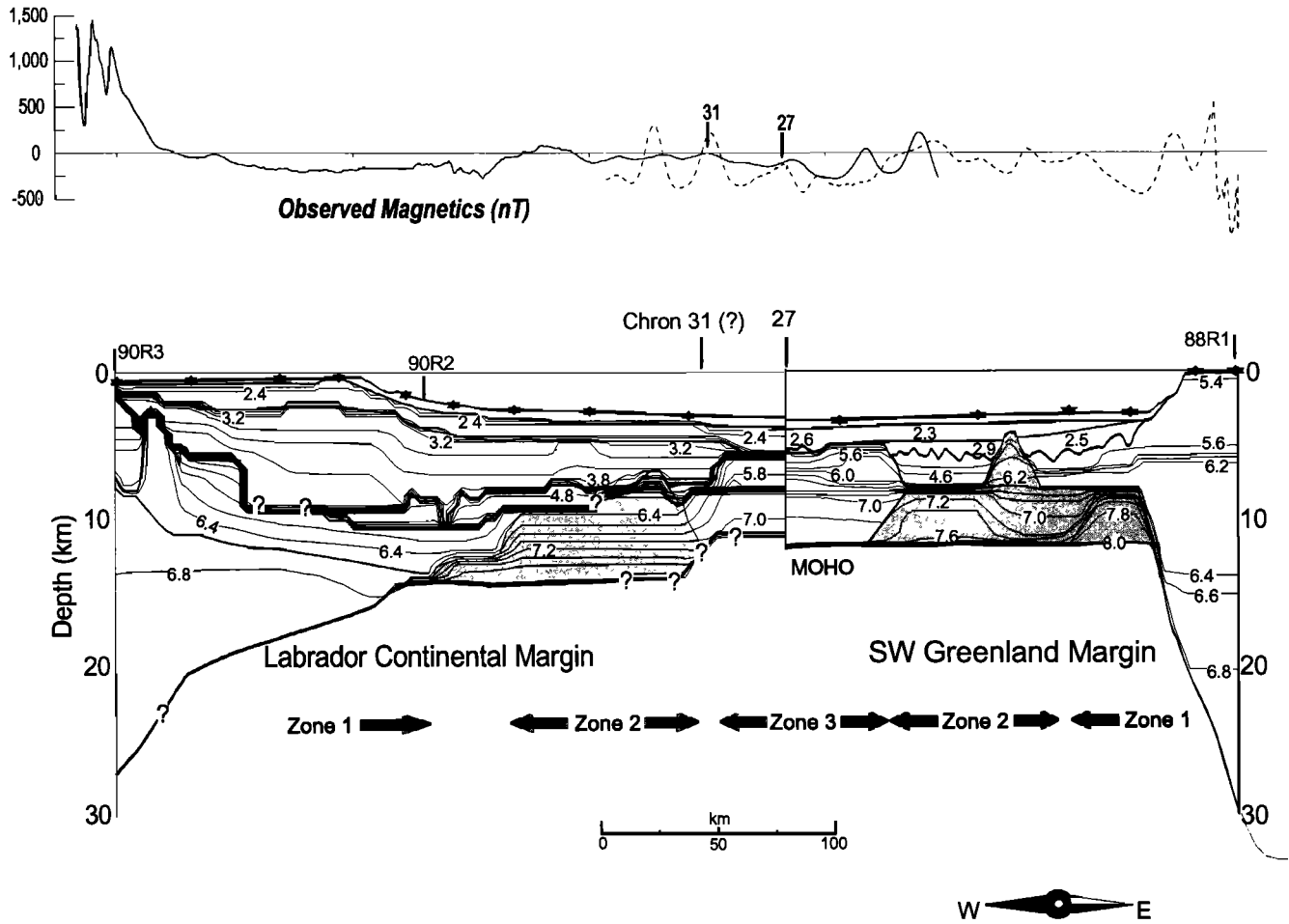
Figure 12. Reconstruction at Chron 27 of magnetic anomaly and crustal velocity contour profiles across the conjugate margins of the Labrador Sea [after *Chian*, 1994]. The Labrador profile is from Figure 10c; the Greenland profile is from *Chian and Louden* [1994]. Note large vertical exaggeration for clarity.

required high asthenospheric temperature will generate a volume of underplate more than 5 times thicker than observed. Reduction of the melt volume by lowering the stretching rate to less than 15 mm/yr [*Bown and White*, 1994] would explain the small volume of melt but is not consistent with the observed high velocity. In the serpentinite model [*Sibuet*, 1992; *Boillot et al.*, 1992], the high-velocity layer is explained by partial serpentinization of mantle peridotite [*Christensen*, 1966; *Fountain and Christensen*, 1989]. This model requires tectonic denudation followed by serpentinization and undercrusting over a wide (70-80 km) area [*Boillot et al.*, 1992] and is supported by ODP sampling at serpentinized peridotite ridges in the Iberia margin [*Boillot et al.*, 1987; *Shipboard Scientific Party*, 1993]. The lack of melt can be attributed to the enhanced conductive cooling due to prolonged continental stretching.

Location. It is difficult for the underplate model to explain why the underplate is offset by ~80 km seaward of, and does not exist beneath, the thinned continental crust where underplating is typically located. A refraction profile located ~500 km north on the western Greenland shelf [*Gohl and Smithson*, 1993], shows a high-velocity (~7.5 km/s) lower crust beneath the shelf which thickens northward from 3 km in the south to 8 km toward Davis Strait, where abundant volcanism occurred at ~Chron 24. It is

reasonable to interpret this northern high-velocity layer as rift-related Mesozoic underplating into the lower continental crust, whereas the high-velocity crust observed in the south is located much farther seaward and was formed before Chron 27. The seaward location of the high-velocity layer is relatively easy to explain as undercrusted serpentinites [*Boillot et al.*, 1989a].

Absence of extrusives and existence of midcrustal reflector. The absence of seaward dipping reflectors [*Balkwill*, 1987] and geochemical signatures [*Clarke et al.*, 1988] indicate an absence of rift-related extrusive volcanics. The existence of an intracrustal reflector [*Keen et al.*, 1994] in zone 2 on the Greenland side but not on the Labrador side can be interpreted as an *S* reflector acting as the seismic signature of a synrift detachment fault, similar to observations from the Bay of Biscay and Galicia Bank margins [*Le Pichon and Barbier*, 1987; *Boillot et al.*, 1992; *Sibuet*, 1992]. In the underplate model, this reflector could be interpreted as the top boundary of melt injection [e.g., *White et al.*, 1994], but in this case it is difficult to explain why it exists only on one side of the conjugate margin pair.

For the above reasons, we conclude that the high-velocity lower crust observed on the conjugate margins of the Labrador Sea is more likely to be serpentinized peridotite rather than underplate.

Upper Crust in the Transition Zone

The upper crust in zone 2 is characterized by a low-velocity layer of 4-5 km/s [*Chian and Louden*, 1994]. This crust appears to be highly faulted on the SW Greenland margin, and its low velocity is compatible with the low-velocity upper crust on the Goban Spur margin [*Horsefield et al.*, 1994], southern Newfoundland margin [*Reid*, 1994], and Flemish Cap margin [*Todd and Reid*, 1989]. An intracrustal reflector is present on the Greenland margin but is not observed in the corresponding zone of the Labrador margin, possibly indicating less velocity contrast between the upper and lower layers.

We do not know the origin of the low-velocity upper crust within the transition zone. The seismic velocity allows several possibilities: altered pillow basalts, upper continental crust, serpentinite, or a mixture of these rocks together with sediment. In the first case, only a small amount of basalt is generated as the top layer of basement over a distance of <200 km (Figure 12). This is consistent with the reinterpreted magnetic anomalies (Chrons 31 and 33) in this zone, even though they are of low amplitude and irregular patterns [*Srivastava and Roest*, 1995]. It is also possible that this material has different origins on the two margins and that the low-velocity upper crust off SW Greenland represents tilted fault blocks of upper continental crust stretched and thinned by a factor of 2-3 [*Chian and Louden*, 1994]. This interpretation can explain the nature of block tilting and existence of the intracrustal reflector for this margin. It is also consistent with the possible absence of more than half of the upper crust on the Labrador margin (Figure 12). The low-velocity upper crust on the Labrador margin is interpreted to be non-continental because no block tilting or intracrustal reflector are observed.

Conclusions

In this paper, we have determined the crustal velocity structure across the Labrador margin from seismic refraction profiles. The results are interpreted in combination with a similarly determined velocity structure across the conjugate SW Greenland margin [*Chian and Louden*, 1994], and data from coincident multichannel reflection, gravity, and magnetic surveys. This constitutes the first detailed crustal velocity analysis for a complete rifted continental margin pair. The results suggest the following:

1. The conjugate margins of the Labrador Sea are divided on each side into three distinct zones according to crustal velocities. Zone 1 represents stretched continental crust, much wider on the Labrador margin than on its conjugate SW Greenland margin. Seaward of this zone, zone 2 is characterized by the existence of a high-velocity (6.4-7.7 km/s) lower crust, nearly symmetrically distributed across both margins over distances of 50-80 km. Farther seaward, zone 3 has typical oceanic crustal velocity, and its age is younger than Chrons 27-31 (62-68 Ma).

2. The continent-ocean transition is best described by the wide zone 2 rather than a sharp boundary. The high-velocity crust in this zone is more likely to be serpentinized peridotite than mafic underplate. This suggests that there was little melt generated in zone 2, which may be explained as a consequence either of a slow rate of continental rifting [*Keen et al.*, 1994; *Bown and White*, 1995] or of tectonic thinning of oceanic crust at a slow rate of seafloor spreading [*Srivastava and Roest*, 1995].

3. The asymmetry in continental thinning across zone 1 indicates that final breakup of the continental crust occurred closer to the Greenland margin. A similar asymmetric location of breakup was determined by *Keen et al.* [1989] between Flemish Cap and

Goban Spur. It is also consistent with predictions of geodynamic models for slow rates of rifting, in which a migration of crustal necking is produced by enhanced cooling and strengthening of the rift zone [*Bassi et al.*, 1993]. A determination of the pre-breakup crustal reconstruction and more complete discussion of the rifting process is presented by *Chian et al.* [1995], using combined data from both refraction and MCS reflection profiles.

References

Balkwill, H.R., Labrador Basin: Structural and stratigraphy style, in Sedimentary Basins and Basin-Forming Mechanisms, edited by C. Beaumont and A.J. Tankard, Can. Soc. Petrol. Geol. Mem., 12, 17-43, 1987.

Bassi, G., Relative importance of strain-rate and rheology for the mode of continental extension, Geophys. J. Int., 122, 195-210, 1995

Bassi, G., C.E. Keen, and P. Potter, Contrasting styles of rifting: Models and examples from the eastern Canadian margin, Tectonics, 12, 639-655, 1993.

Bell, J.S. (Coordinator), East Coast Basin Atlas Series, Labrador Sea, Atlantic Geosci. Cent., Geol. Surv. of Can., Dartmouth, Nova Scotia, 1989.

Boillot, G., et al., Tectonic denudation of the upper mantle along passive margins: A model based on drilling results (ODP Leg 103, western Galicia margin, Spain); Tectonophysics, 132, 335-342, 1987.

Boillot, G., J., G. Feraud, M. Recq, and J. Girardeau, "Undercrusting" by serpentinite beneath rifted margins: The examples of the west Galicia margin (Spain), Nature, 341, 523-525, 1989a.

Boillot, G., D. Mougenot, J. Girardeau, and E.L. Winterer, Rifting processes on the west Galicia margin, Spain, in Extensional Tectonics and Stratigraphy of the North Atlantic Margins, edited by A.J. Tankard and H.R. Balkwill, Tulsa, Okla., AAPG Mem., 46, 363-377, 1989b.

Boillot, G., J., M.O. Beslier, and M. Comas, Seismic image of undercrusted serpentinite beneath a rifted margin, Terra Nova, 4, 25-33, 1992.

Bown, J.W., and R.S. White, Variation with spreading rate of oceanic crustal thickness and geochemistry, Earth Planet. Sci. Lett., 121, 435-449, 1994.

Bown, J.W., and R.S. White, The effect of finite extension rate on melt generation at rifted continental margins J. Geophys. Res., in press, 1995.

Cerveny, V., I.A. Molotkov, and I. Psencik, Ray Method in Seismology, 214 pp., Univ. of Karlova, Prague, 1977.

Chalmers, J.A., New evidence on the structure of the Labrador Sea/Greenland continental margin, J. Geol. Soc., London, 148, 899-908, 1991.

Chalmers, J.A., and K.H. Laursen, Labrador Sea: The extent of continental and oceanic crust and the timing of the onset of seafloor spreading, Mar. Pet. Geol., 12, 205-217, 1995.

Chian, D., The conjugate margins of the Labrador Sea: Crustal structure from refraction profiles and their tectonic implications, Ph.D. thesis, 233 pp., Dalhousie Univ., Halifax, Nova Scotia, 1994.

Chian, D., and K.E. Louden, The structure of Archean/Ketilidian crust along the continental shelf of southwestern Greenland from a seismic refraction profile, *Can. J. Earth Sci., 29,* 301-313, 1992.

Chian, D., and K.E. Louden, The continent-ocean crustal transition across the southwest Greenland margin, *J. Geophys. Res., 99,* 9117-9135, 1994.

Chian, D., C. E. Keen, I. Reid, and K.E.Louden, Evolution of non-volcanic rifted margins: New results from the conjugate margins of the Labrador Sea, *Geology,* 23, 589-1995.

Christensen, N.I., Elasticity of ultramafic rocks, *J. Geophys. Res., 71,* 5921-5931, 1966.

Clarke, D. B., B.I. Cameron, G.K. Muecke, and J.L. Bates, Early Tertiary basalts from the Labrador Sea floor and Davis Strait region, *Can. J. Earth Sci., 26,* 956-968, 1988.

Fountain, D M., and N.I. Christensen, Composition of the continental crust and upper mantle: A review, in *Geophysical Framework of the Continental United States,* edited by L.C. Pakiser and W.D. Mooney, *Mem. Geol. Soc. Am.,* 172, 711-742, 1989.

Furlong, K. P., and D.M. Fountain, Continental crustal underplating: Thermal considerations and seismic-petrologic consequences. *J. Geophys. Res., 91,* 8285-8294, 1986

Gohl, K., and S.B. Smithson, Structure of Archean crust and passive margin of southwest Greenland from seismic wide-angle data, *J. Geophys. Res., 98,* 6623-6638, 1993.

Horsefield, S.J., R.B. Whitmarsh, R.S. White, and J.-C. Sibuet, Crustal structure of the Goban Spur passive continental margin Results of a detailed seismic refraction survey, *Geophys. J. Int., 119,* 1-19, 1994.

Keen, C.E., C. Peddy, B. de Voogd, and D. Matthews, Conjugate margins of Canada and Europe: Results from deep reflection profiling, *Geology, 17,* 173-176, 1989.

Keen, C.E., P. Potter, and S.P. Srivastava, Deep seismic reflection data across the conjugate margins of the Labrador Sea, *Can. J. Earth Sci., 31,* 192-205, 1994.

Kent, D.V., and F.M. Gradstein, F.M., A Jurassic to recent chronology, in *The Geology of North America,* vol. M, *The Western North Atlantic Region,* edited by P.R. Vogt and B E. Tucholke, pp. 379-404, Geol. Soc. of Am., Boulder, Colo., 1986.

Le Pichon, X., and F. Barbier, Passive margin formation by low-angle faulting with the upper crust: The northern Bay of Biscay margin, *Tectonics, 6,* 133-150, 1987.

Lister, G.S., M.A Ethridge, and P.A. Symonds, Detachment faulting and the evolution of passive continental margins, *Geology, 14,* 246-250, 1986.

Ludwig, W.J., J.E. Nafe, and C.L. Drake, Seismic refraction, in *The Sea,* vol. 4, edited by A.E. Maxwell, pp. 53-84, Wiley-Interscience, New York, 1971.

McKenzie, D.P., Some remarks on the development of sedimentary basins, *Earth Planet. Sci. Lett., 40,* 25-32, 1978.

Pinheiro, L.M., R.B. Whitmarsh, and P.R. Miles, The ocean-continent boundary off the western continental margin of Iberia, II, Crustal structure in the Tagus Abyssal Plain, *Geophys J. Int., 109,* 106-124, 1992

Reid, I.D., Crustal structure of a nonvolcanic rifted margin east of Newfoundland, *J. Geophys. Res., 99,* 15161-15180, 1994.

Reid, I. D., and H R. Jackson, Oceanic spreading rate and crustal thickness; *Mar. Geophys. Res., 5,* 165-172, 1981.

Reid, I.D., and C.E. Keen, High seismic velocities associated with reflections from within the lower oceanic crust near the continental margins of eastern Canada, *Earth Planet. Sci. Lett., 99,* 118-126, 1990

Roest, W.R., and S. P. Srivastava, Sea-floor spreading in the Labrador Sea: A new reconstruction, *Geology, 17,* 1000-1003, 1989.

Rolle, F., Late Cretaceous-Tertiary sediments offshore central west Greenland: Lithostratigraphy, sedimentary evolution and petroleum potential, *Can. J. Earth Sci., 22,* 1001-1019, 1985.

Shipboard Scientific Party, ODP drills the west Iberia rifted margin, *ES Trans. AGU, 74,* 454-455, 1993.

Sibuet, J.-C., Formation of nonvolcanic passive margins: A composite model applied to the conjugate Galicia and southeastern Flemish Cap margins, *Geophys. Res. Lett., 19,* 769-772, 1992.

Srivastava, S.P., Evolution of the Labrador Sea and its bearing on the early evolution of the North Atlantic, *Geophys. J. R. Astron. Soc., 52,* 313-357, 1978.

Srivastava, S. P., and W. R. Roest, Nature of thin crust across the southwest Greenland margin and its bearing on the location of the ocean-continent boundary, in *Rifted Ocean-Continent Boundaries,* edited by E. Banda, M. Torne, and M. Talwani, pp.95-120, Kluwer Academic Publishers, Mallorca (Spain), 1995.

Stergiopolous, A B., Geophysical crustal studies off the southwest Greenland margin, M.Sc. thesis, 250 pp., Dalhousie Univ., Halifax, Nova Scotia, 1984.

Todd, B.J., and I. Reid, The continent-ocean boundary south of Flemish Cap: Constraints from seismic refraction and gravity, *Can. J. Earth Sci., 26,* 1392-1407, 1989.

Tucholke, B., Sediment distribution, in *Geophysical Atlas of the North Atlantic Between 50° to 72° N and 0° to 65° W,* edited by S.P Srivastava, D. Voppel, and B. Tucholke, pp. 9-12, Dsch. Hydrog. Inst., Hamburg, 1988.

Van der Linden, W.J.M., Crustal attenuation and sea-floor spreading in the Labrador Sea, *Earth Planet. Sci Lett., 27,* 409-423, 1975

Watt, W.S., The coast-parallel dike swarm of southwest Greenland in relation to the opening of the Labrador Sea, *Can. J. Earth Sci., 6,* 1320-1321, 1969.

Wernicke, B., Uniform-sense normal simple shear of the continental lithosphere, *Can. J Earth Sci., 22,* 108-125, 1985.

White, R., and D McKenzie, Magmatism at rift zones: The generation of volcanic continental margins and flood basalts, *J. Geophys. Res., 94,* 7685-7729, 1989.

White, R.S., J H. McBride, T.J. Henstock, and R.W. Hobbs, Internal structure of a spreading segment of Mesozoic oceanic crust, *Geology, 22,* 597-600, 1994.

Whitmarsh, R. B., F. Avedik, and M.R. Saunders, The seismic structure of thinned continental crust in the northern Bay of Biscay, *Geophys J. R. Astron. Soc., 86,* 589-602, 1986.

Whitmarsh, R.B., P.R. Miles, and A. Mauffret, The ocean-continent boundary off the western continental margin of Iberia, I, Crustal structure at 40°30'N, *Geophys. J. Int., 103,* 509-531, 1990.

Whitmarsh, R.B., L.M. Pinheiro, P.R. Miles, M. Recq, and J.-C. Sibuet, Thin crust at the western Iberia ocean-continent transition and ophiolites, *Tectonics, 12,* 1230-1239, 1993.

D. Chian and I. Reid, Geological Survey of Canada (Atlantic), Bedford Institute of Oceanography, Dartmouth, Nova Scotia, Canada B2Y 4A2.

K. E. Louden, Department of Oceanography, Dalhousie University, Halifax, Nova Scotia, Canada B3H 4J1. (e-mail: keith@papa.ocean.dal.ca)